

# Morphological deficiency in the prenatal anterior cranial base of midfacially retrognathic mice

WENBIN MA AND SCOTT LOZANOFF

Departments of Anatomy and Oral Biology, University of Saskatchewan, Saskatoon, Saskatchewan, Canada

(Accepted 14 November 1995)

---

## ABSTRACT

The role of the anterior cranial base in the establishment of midfacial retrognathia remains unclear. The purpose of this study was to determine whether morphological deficiencies occur in the developing anterior cranial base of the retrognathic Brachyrrhine (3H1 *Br/+*) mouse mutant shortly after overt cartilaginous differentiation and to localise any malformations. Crania from 2 groups of 3H1 *Br/+* and *+/+* mice, each consisting of 15 animals, were collected at gestational days 15, 17 and 19 (Theiler stages 23, 25, 27). The anterior cranial base from each specimen was subjected to computerised reconstruction and 8 homologous anatomical landmarks were digitised on each model. The landmark configurations were subjected to Procrustes analysis and significant differences between models were determined at each age. In order to localise differences between forms, average landmark configurations derived from Procrustes analysis were subjected to finite-element analysis. Two cluster models were generated based on size-change values. One cluster was located anteriorly and superiorly while the second was located posteriorly and inferiorly within the anterior cranial base. Results indicate that the size-change values for the posterior and inferior cluster increased more rapidly compared with the anterior and superior region over the age range tested. These data indicate that the midfacial retrognathia in *Br/+* mice is associated with abnormal growth activity in the presphenoid component of the presumptive anterior cranial base. In addition, the deficiency is present in the presphenoid at the time of overt cartilaginous differentiation.

*Key words:* Brachyrrhine mutant mouse; finite element analysis.

---

## INTRODUCTION

The anterior cranial base forms the central stem of the cranium and includes the cartilaginous nasal septum, perpendicular plate of the ethmoid, vomer and sphenoidal body in the adult skull. Additionally, the sphenoid is divided into the presphenoid, extending anteriorly from the clivus, and the postsphenoid, continuing posteriorly to the spheno-occipital junction. In the mouse, the anterior cranial base, with the exception of the vomer which forms intramembranously, begins to chondrify at E12 (Theiler stage 20), but does not achieve its mature cartilaginous configuration until E15 (Theiler stage 23). The anterior cranial base is considered to play an important role in the emergence of prenatal midfacial morphology since the nasomaxillary complex is fixed to it. In addition, the anterior cranial base displays

dramatic growth activity during the late embryonic and early fetal periods prior to the extensive formation of the craniofacial bones (Burdi, 1969, 1976*a, b*; Van Limborgh, 1970, 1972; Diewert, 1983, 1985; Burdi et al. 1988). However, its specific role in the aetiology of midfacial dysmorphologies remains debated (Ross, 1965, 1987; Dahl, 1970; Sandham & Cheng, 1988; Horswell & Gallup, 1992; Harris, 1993; Trotman & Ross, 1993).

Recently, a mouse mutant (Brachyrrhine, *Br*) was identified which shows midfacial retrognathia characteristic of a Class III malocclusion in humans (Lozanoff, 1993). The mouse mutant was developed in order to determine the effects of neutron irradiation on chromosome structure (Searle, 1966). Adult *Br/+* heterozygotes display severe midfacial hypoplasia and deficiencies in midfacial calcification while median midfacial clefting occurs in the dominant homozygote

condition. Midfacial retrognathia is recognizable externally as early as 15 d of gestation (Theiler stage 23) and the malformation is independent of fetal blebbing which causes embryonic malformations in over-irradiated mice due to mechanical disruption (Ma & Lozanoff, 1993). Lozanoff et al. (1994) showed that the anterior cranial base is deficient in early postnatal *Br* mice with the presphenoid being most affected, while the sphenothmoidal area was affected secondarily and the precursor region of the cartilaginous nasal septum was least affected. The purpose of this study is to determine whether the midfacially retrognathic condition in *Br*/+ mice is associated with anterior cranial base malformations during early embryonic development, particularly in the period of overt cartilaginous differentiation and, if so, to localise the deformity.

#### MATERIALS AND METHODS

Inbred adult C3H/He × 101/H (3H1) stock and *Br* mice were purchased from Harwell Laboratories (MRC), Oxford, UK, and these were used to establish a breeding colony in our laboratory (Lozanoff, 1993). The 3H1 *Br*/+ mice were compared with a sample of 3H1 +/+ stock mice since these animals display normal murine craniofacial morphology. All animals were housed under standard conditions with a 12 h light cycle. They were supplied with tap water and food pellets (Agway Prolab Feed, Waverly, NY) ad libitum. The *Br* mice display incisors that grow very rapidly and do not wear normally, probably due to malocclusion resulting from their abnormal midfacial condition. Therefore, the incisors were trimmed manually with scissors once every 2 wk. The food pellets were broken into smaller pieces than was available commercially in order to facilitate ingestion. However, animals were handled equivalently in all other respects. Random breeding of *Br* mice was conducted by placing 2 nulliparous 3H1 stock females with a singly caged *Br* male. Parturition occurred during the night and embryos were designated as gestational day 0 (E0) the following morning. Mice were identified as *Br* if they showed midfacial retrusion and renal hypoplasia which are 2 morphological markers which provide accurate discrimination between *Br*/+ and +/+ littermates (Ma & Lozanoff, 1993). The +/+ control sample was derived from 3H1 stock matings.

Nonlittermates were collected at E15 (stage 23), E17 (stage 25) and E19 (stage 27). Dams were killed with a lethal dose of Metofane (methoxyflurane), embryos were removed, killed and staged according to

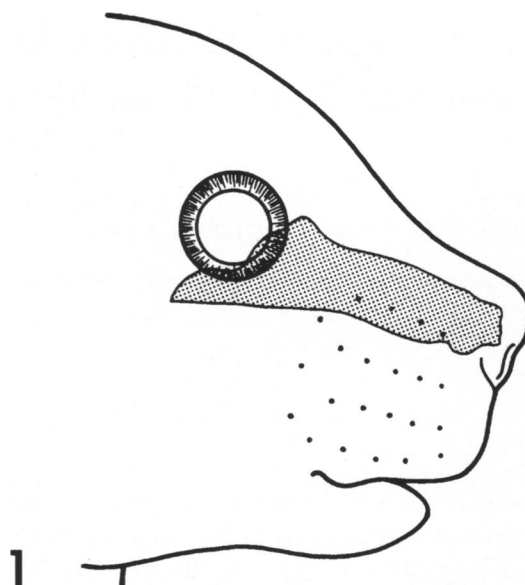


Fig. 1. Schematic representation of the murine anterior cranial base.

Table 1. Anatomical landmarks used in the analysis

| Landmark number | Description                                                                                                        |
|-----------------|--------------------------------------------------------------------------------------------------------------------|
| 1               | Most anterior point at the junction between the right superior limb of cupula anterior and the nasal septum.       |
| 2               | Most anterior point at the junction between the left superior limb of cupula anterior and the nasal septum.        |
| 3               | Most anterior point at the junction between the left inferior limb of cupula anterior and the nasal septum.        |
| 4               | Most anterior point of the junction between the right inferior limb of cupula anterior and the nasal septum.       |
| 5               | Base of crista galli on the right side.                                                                            |
| 6               | Base of crista galli on left side.                                                                                 |
| 7               | Most posterior point at the junction between the cupula posterior and the anterior cranial base on the left side.  |
| 8               | Most posterior point at the junction between the cupula posterior and the anterior cranial base on the right side. |

Theiler (1989). Eight specimens were collected for each age and facial condition and at least 5 embryos per age/facial condition were used in the subsequent analysis. Heads were fixed in 2% glutaraldehyde in 0.05 M cacodylate buffer for 3–4 d. Following fixation, they were washed in water, decalcified with RDO (Ingram Bell) and stored in neutral phosphate buffer for approximately 1 wk. The cartilaginous anterior cranial base is shown schematically in Figure 1 in order to provide an anatomical reference. The anterior cranial base from each individual was reconstructed

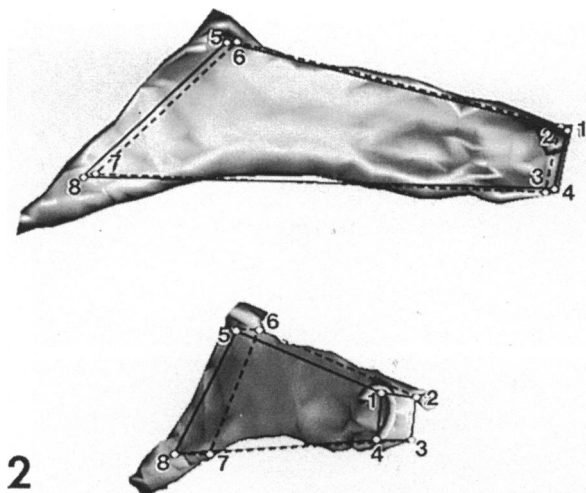


Fig. 2. Computerised reconstruction of the anterior cranial base of the mouse viewed from the right lateral and anterolateral perspectives with the 8 homologous landmarks used in this analysis.

and viewed following Lozanoff (1992). This technique provides precise models of the anterior cranial base in mice. Volumes and surface areas for each model also were calculated (Lozanoff & Deptuch, 1991). Volumes were compared between facial conditions at each age using a paired *t* test.

Each reconstruction was viewed on the monitor from lateral, superior, inferior, and posterior perspectives and compared qualitatively. Eight homologous anatomical landmarks (Table 1) were identified on the models (Fig. 2). These landmarks were selected since they represented anatomical features that were easily recognisable on all models and they were located with a high degree of accuracy (Lozanoff et al. 1994). Landmarks were digitised by rotating each reconstruction to a standardised lateral position. Then, the cursor was positioned on the reconstruction and a ray was projected perpendicularly through the model. The first surface triangle intersected by the ray was identified and the point of intersection provided the 3-dimensional coordinate for the landmark. Individual landmark configurations were used to calculate average models for each age group (E15, E17, E19) and craniofacial type (3H1 *+/+* or *Br/+*) using Procrustes analysis which superimposed all specimens at their geometric centres (Gower, 1975; Rohlf & Slice, 1990). The 95% confidence intervals for the nodal locations were generated and displayed at each of the 8 landmarks in order to determine whether positional variation was qualitatively similar between models and within age groups. Average configurations were compared for each age and facial condition in order to determine whether the *Br/+* models were significantly different from the cor-

responding *+/+* averages. Euclidean Distance Matrix Analysis (EDMA) also was used to determine whether average geometries differed between 3H1 *+/+* and *Br/+* groups following Lele (1993).

Average configurations were analysed with finite-element methods for samples determined to be significantly different from one another in order to localise differences in anatomical form (Lozanoff et al. 1994). The average 3H1 *Br/+* geometry was used as the initial form and compared with the 3H1 *+/+* mean configuration for each developmental stage. The 3 principal stretches at each point were multiplied together providing a measure of change in local size (Lozanoff & Diewert, 1989). These size-change values were measured at 500 randomly selected points within the *Br/+* model for each age group, plotted within the model and viewed from various perspectives, but only the lateral view is provided in this report.

The size variables within each model were subjected to k-means cluster analysis based on their magnitude and location (Johnson & Wichern, 1982, pp. 555–558). Resulting clusters were plotted graphically within the *Br/+* (initial) geometry and tested for significance following Duda & Hart (1973). The analysis began by testing for 2 significantly different clusters and the number of clusters were incremented by 1 until the hypothesis that independent clusters existed was rejected (Lozanoff et al. 1994). Average size-change values and corresponding standard deviations were calculated for each cluster determined to be significantly different from the others and tabulated for each finite-element comparison.

## RESULTS

Representative models of the anterior cranial base for *Br/+* and *+/+* mice at E15 (stage 23), E17 (stage 25) and E19 (stage 27) are provided in Figure 3. The overall size of the anterior cranial base appeared similar between normal and *Br/+* animals at E15, but the presphenoidal region in the 3H1 *Br/+* specimens appeared much smaller (Fig. 3). The sphenothmoidal region of the 3H1 *Br/+* specimens, positioned superiorly in the region of the crista galli, appeared reduced in size compared with the same area in the 3H1 *+/+* models (Fig. 3). By E17, the 3H1 *+/+* specimens appeared larger than the mutants (Fig. 3). The anterior region of the anterior cranial base in the 3H1 *Br/+* specimens appeared normal in form compared with the 3H1 *+/+* models at this age; however, the presphenoidal and sphenothmoidal regions were noticeably smaller in the mutants (Fig.

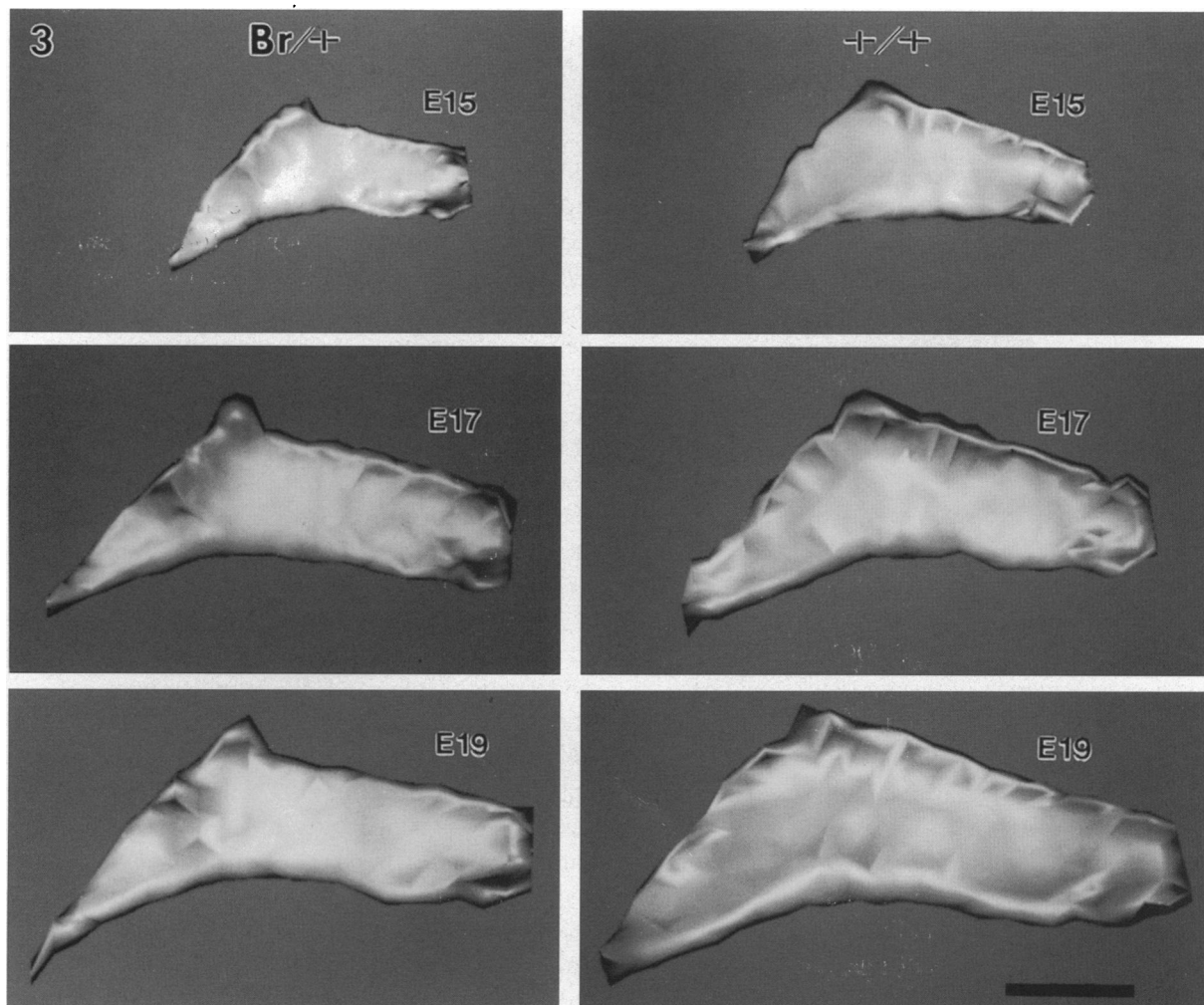


Fig. 3. Computerised models of the anterior cranial base from representative 3H1 *Br/+* and *+/+* animals at E15, E17 and E19 viewed from the right lateral perspective. Bar, 1.0 mm.

Table 2. Comparison of anterior cranial base volumes ( $\text{mm}^3$ ) between 3H1 *+/+* and *Br/+* mice at days 15 (E15), 17 (E17) and 19 (E19)\*

| Age | 3H1 <i>Br/+</i> | 3H1 <i>+/+</i> | P      |
|-----|-----------------|----------------|--------|
| E15 | 0.241 (0.015)   | 0.268 (0.024)  | NS     |
| E17 | 0.576 (0.068)   | 0.667 (0.100)  | NS     |
| E19 | 0.783 (0.091)   | 1.054 (0.224)  | < 0.01 |

\* Means (S.D.)

3). This trend continued for the E19 comparison (Fig. 3).

The volumes of the *Br/+* anterior cranial bases were smaller, but not statistically significant, compared with normal mice at E15 and E17 (Table 2). However, the anterior cranial base volumes were significantly smaller in *Br* mutants compared with the normals at E19 (Table 2).

Average geometries for the anterior cranial bases from 3H1 *+/+* and *Br/+* animals from each age group, generated from the Procrustes analysis, are provided in Figure 4. Variation in landmark location is represented at each node by 95% confidence ellipsoids. Variation in the landmark positions for the mean geometries of all groups appeared relatively small (Fig. 4). However, landmark variation appeared greater for 3H1 *Br/+* mice compared with the normal, particularly at 19 d gestation. A comparison of residuals derived from Procrustes analysis showed that the 3H1 *Br/+* models were significantly different ( $P < 0.001$ ) from those of the *+/+* animals at all age intervals (Table 3). In addition, results from the EDMA analysis showed that the 3H1 *+/+* and *Br/+* groups were significantly different at  $P < 0.01$ .

Maps of local changes in size derived from finite-element comparisons between 3H1 *Br/+* and *+/+* are given in Figure 5 and numerical data associated

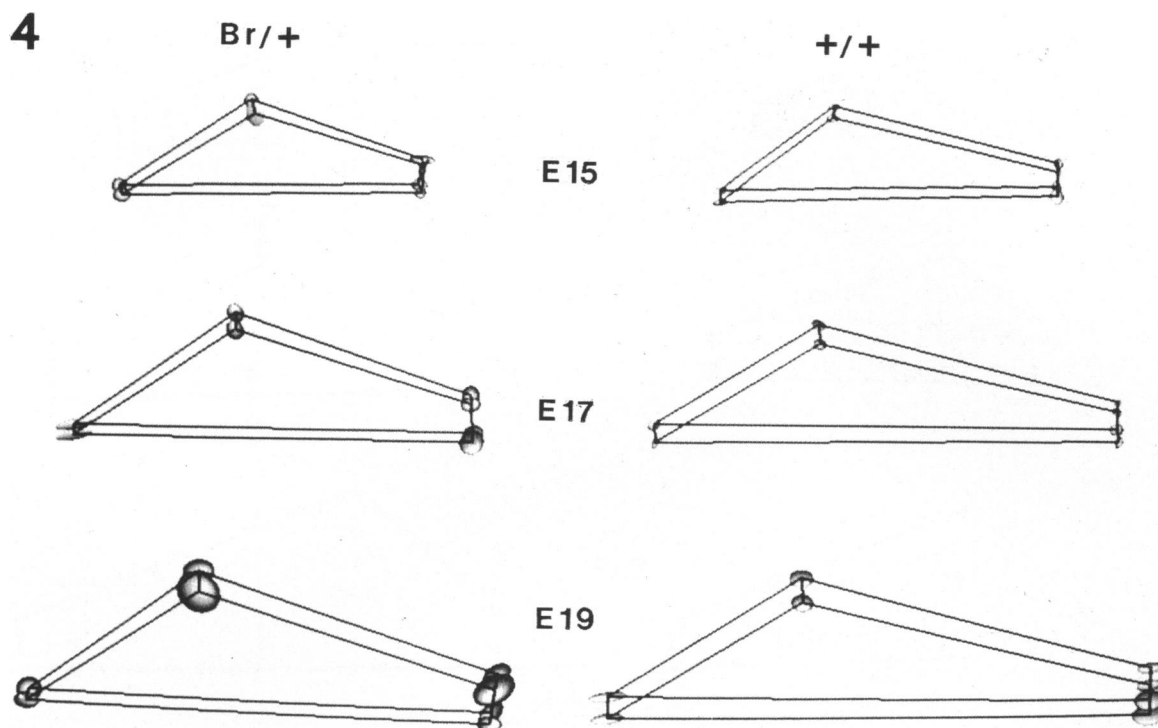


Fig. 4. Average geometries for 3H1 *Br/+* and *+/+* groups at E15, E17 and E19 viewed from the right lateral perspective with 95% confidence intervals for landmark locations indicated by ellipsoids.

Table 3. Comparison of 3H1 *+/+* and *Br/+* anterior cranial base models at days 15 (E15), 17 (E17) and 19 (E19) gestation and probability of geometric equivalence based on Procrustes analysis

| Age | Residual | F value | P value |
|-----|----------|---------|---------|
| E15 | 0.00147  | 17.4    | < 0.001 |
| E17 | 0.00093  | 39.9    | < 0.001 |
| E19 | 0.00679  | 17.1    | < 0.001 |

with these models in Table 4. At 15 d gestation, the size-change values separated discretely into 2 clusters for the 3H1 *Br/+* and *+/+* comparison with 1 cluster of smaller size-change occurring superiorly, while a second cluster of larger size-change values existed inferiorly and slightly posteriorly (Fig. 5). Size change-values clustered into 2 discrete groups for the E17 anterior cranial base comparison, one with smaller values located anteriorly and superiorly and a second cluster, located posteriorly and inferiorly, with larger values (Fig. 5). Similarly, size-change values clustered into 2 groups for the comparison of anterior cranial base models for the 19 d gestational groups with the posterior and inferior region displaying a larger average compared with the anterior and superior region (Fig. 5). Within all age categories, the 2 clusters were significantly different from one another with the posterior and inferior cluster displaying

larger local size-change values compared with the anterior and superior cluster (Table 4). A ratio criterion test (Duda & Hart, 1973; Lozanoff et al. 1994) was performed to determine whether the size-change values could be further subdivided into 3 clusters; however, statistical significance did not occur with further cluster subdivisions.

In general, size-change values clustered into 2 groups for the 3H1 *Br/+* geometries when compared with the 3H1 *+/+* geometries, one located posteriorly and inferiorly with the other positioned anteriorly and superiorly. Average size-change values for the posteroinferior cluster were larger compared with the anterosuperior cluster over the age range tested. Further subdivision of the clusters was not statistically significant.

#### DISCUSSION

Qualitative and quantitative analyses of computerised morphological reconstructions are becoming increasingly useful in the study of craniofacial growth and malgrowth (Siegel & Todhunter, 1979; Mooney et al. 1991; Lozanoff et al. 1993; Witt et al. 1992; Lozanoff et al. 1994; Rudé et al. 1994; Sameshima & Melnick, 1994). The technique used here has been shown to provide accurate and precise models of the murine anterior cranial base (Lozanoff, 1992). As well, an assessment of nodal residuals within indi-

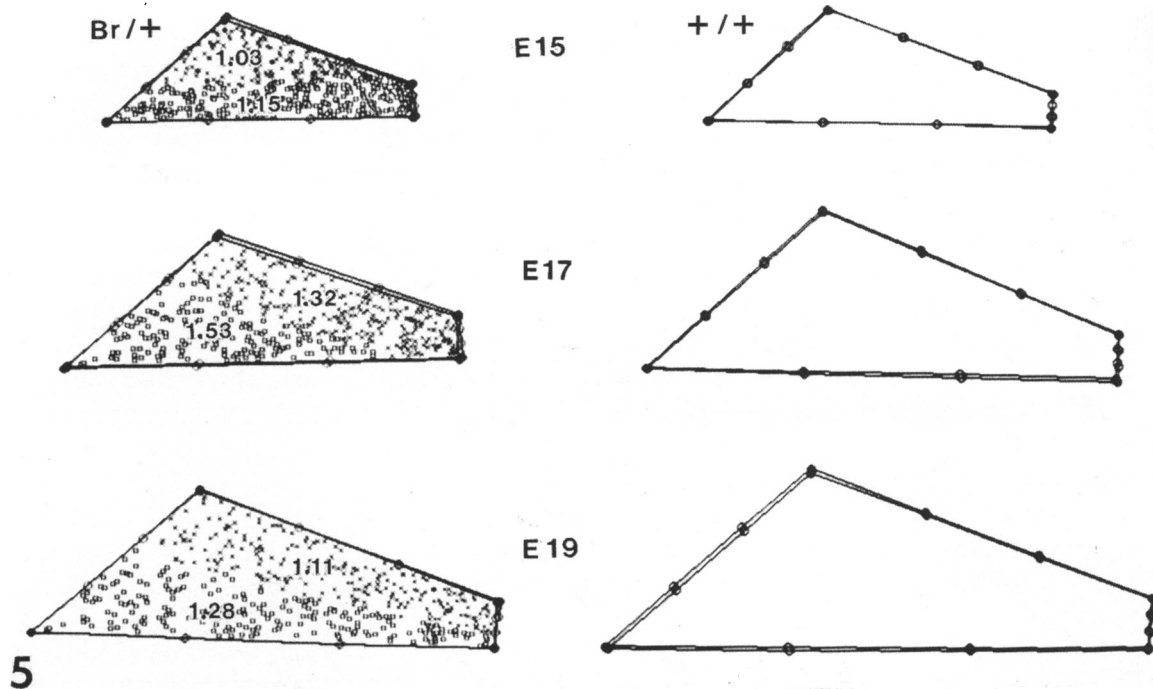


Fig. 5. Finite element comparison of *Br/+* and *+/+* average geometries at days 15 (E15), 17 (E17) and 19 (E19) gestation with mean size-change values plotted within the respective clusters.

Table 4. Comparison of local size-change values derived from the finite-element analysis of average anterior cranial base geometries from 3H1 *+/+* and *Br/+* animals at days 15 (E15), 17 (E17) and 19 (E19) gestation

| Age | A         |      | P         |      | P value |
|-----|-----------|------|-----------|------|---------|
|     | $\bar{x}$ | S.D. | $\bar{x}$ | S.D. |         |
| E15 | 1.03      | 0.06 | 1.15      | 0.05 | < 0.001 |
| E17 | 1.32      | 0.05 | 1.53      | 0.10 | < 0.001 |
| E19 | 1.11      | 0.04 | 1.28      | 0.08 | < 0.001 |

A, anterosuperior cluster; P, posteroinferior cluster.

viduals versus that within group suggests that anatomical landmarks can be identified in a reliable fashion, although the analysis of landmark precision remains problematic (Lozanoff et al. 1994). The usefulness of finite-element modelling for measuring anatomical change remains debated (Bookstein, 1991; McAlarney et al. 1991, 1992). However, Lozanoff & Diewert (1986) demonstrated that form-change variables derived from finite-element modelling do correspond to drug-induced craniofacial malgrowth alterations in a predictable fashion. Therefore, finite-element descriptions of dysmorphology in the murine anterior cranial base appear to provide accurate and reliable information.

Adult 3H1 *Br* mice display severe midfacial retrognathia (Lozanoff, 1993). Similarly, young postnatal

*Br* mice show midfacial retrognathia externally and a deficient anterior cranial base internally (Lozanoff et al. 1994). In this study, prenatal mutants displayed anterior cranial bases with smaller volumes, but not statistically significantly less, compared with 3H1 *+/+* at 15 d gestation which is approximately 3 d subsequent to the initiation of chondrification in the murine anterior cranial base. This trend continues until 17 d gestation, after which the volume of the *Br/+* anterior cranial base is statistically significantly less compared with the normal organ. However, the geometric configuration of the *Br/+* anterior cranial base differs from the normal throughout the age range tested, based on Procrustes analysis and EDMA. Therefore morphological deficiencies in the anterior cranial base of the *Br/+* mouse that are seen postnatally (Lozanoff et al. 1994) arise very early in development, possibly at the onset of chondrification.

The anterior cranial base forms from the central stem of the chondrocranium and this single cartilaginous structure undergoes divergent morphogenetic processes to form the cartilaginous nasal septum as well as the bony perpendicular plate of the ethmoid, presphenoid, postsphenoid and basisphenoid bones. During the ossification process, chondrocytic hypertrophy occurs along a posterior to anterior axis, with the anterior portion remaining cartilaginous and forming the nasal septum. Based on the results from the finite-element analysis, the size-change values

clustered discretely into 2 groups, one located posterior and inferior and the other anterior and superior when the *Br/+* average models were compared with the 3H1 *+/+* average configurations. In addition, the average size-change values were larger for the posterior cluster compared with the anterior cluster. These results indicate that growth activity in the presphenoidal region, inferiorly, ascending to the sphenothmoidal region, superiorly, is probably affected more than the presumptive cartilaginous nasal septum. Delayed growth could also be expected in the *Br* mouse along the ossifying front of the presphenoid, extending from the base of the sphenoid superiorly to the crista galli.

A short anterior cranial base has been implicated as a factor in Class III malocclusions resulting in midfacial retrognathia (Stapf, 1948; Moss & Greenberg, 1955; Hopkin et al. 1968). Numerous hypotheses have been proposed regarding the relationship between longitudinal growth of the anterior cranial base and midfacial retrognathia. Among these, the traction hypothesis postulates that the nasal septum pulls the midfacial skeleton forwards through the septopremaxillary ligament (Scott, 1953; Latham, 1970; Sarnat, 1970; Delaire & Precious, 1986; Mooney et al. 1989). Experimental evidence indicates that a disruption in the septopremaxillary ligament results in midfacial retrusion (Sarnat, 1991; Siegel et al. 1991, 1992). However, a greater reduction in local size occurring in the presphenoidal and sphenothmoidal regions of the *Br* anterior cranial base compared with that seen in the nasal septal region could result in midfacial retrognathia as seen in the present study. The posterior region of the anterior cranial base may be more significant compared with the nasal septal region for causing midfacial retrognathia in the *Br* mutant.

Sagittal growth of the cranial base is accomplished at numerous sites along its length (Hoyte, 1991). Of particular significance are the sphenoccipital synchondrosis and the synchondroses of the coronal ring (Burdi et al. 1986). The defective morphology in the presphenoid extending superiorly towards the sphenothmoidal region probably prevents proper midfacial prognathism as seen in *Br* embryos (Ma & Lozanoff, 1993). The cellular deficiency responsible for this decreased growth is still unknown. It is possible that there is a deficient embryonic aggregate of prechondrocytes resulting in a reduced stem cell population and a small presphenoid. Alternatively, the prechondrogenic cell population may differentiate properly. However, the chondrocytes may mature too rapidly, limiting necessary growth activities such as extra-

cellular matrix production and cellular proliferation, to ensure proper longitudinal growth. This process may occur in Apert's syndrome where the sphenoccipital synchondroses may fuse prematurely, or remain open, but with diminished growth activity (Kreiborg et al. 1976; Ousterhout & Melsen 1982). Future work will attempt to elucidate the cellular mechanisms associated with foreshortening of the cranial base in *Br* mice.

Approximately 20–30% of adult patients with Class III malocclusions display maxillary retrognathia without mandibular prognathism (Sanborn, 1955; Dietrich, 1970; Jacobson et al. 1974; Ellis & McNamara 1984). The malocclusion can be recognised clinically in young patients aged as early as 5–7 y (Guyer et al. 1986). In patients younger than 8 y, Singh et al. (1995) showed that a localised morphological shearing occurs in the presphenoidal and sphenothmoidal regions of the cranial base in Class III patients. This suggests that abnormal growth occurs locally within the presphenoidal area in human patients. In the present study, results from the FEM analysis suggest that growth activity in the anterior cranial base may be divisible into 2 regions; one located anteriorly in the presumptive nasal septal region and the other positioned posteriorly in the presphenoidal area extending superiorly into the sphenothmoidal region. Growth deficiencies in the presphenoidal region, rather than the nasal septum, appear to cause midfacial retrognathia as seen in *Br/+* mice.

#### ACKNOWLEDGEMENTS

Dr Mengjing Yu and Mr John Deptuch provided technical assistance in this study. Dr T. Cole provided the EDMA routine as well as helpful suggestions regarding its implementation. Supported by MRC-MT-10269 (S.L.) and a College of Medicine Graduate Research Scholarship (W.M.).

#### REFERENCES

- BOOKSTEIN FL (1991) *Morphometric Tools for Landmark Data*. Cambridge: Cambridge University Press.
- BURDI AR (1969) Cephalometric growth analysis of the human upper face region during the last two trimesters of gestation. *American Journal of Anatomy* **125**, 133–142.
- BURDI AR (1976a) Biological forces that shape the human midface before birth. In *Factors Affecting the Growth of the Midface* (ed. J. A. McNamara), pp. 9–42. Craniofacial Growth Series, Monograph 6. Ann Arbor: University of Michigan.
- BURDI AR (1976b) Early development of the human basicranium: its morphogenetic controls, growth patterns, and relations. In *Symposium on Development of the Basicranium* (ed. J. F. Bosma), pp. 81–90. Bethesda: DHEW Publication No. 76-989.
- BURDI AR, KUSNETZ AB, VENES JL, GEBARSKI SS (1986) The



- natural history and pathogenesis of the cranial coronal ring articulations: implications in understanding the pathogenesis of Crouzon craniostenotic defects. *Cleft Palate Journal* **23**, 28–38.
- BURDI AR, LAWTON TJ, GROSSLIGHT J (1988) Prenatal pattern emergence in early human facial development. *Cleft Palate Journal* **25**, 8–15.
- DAHL E (1970) Craniofacial morphology in congenital clefts of the lip and palate. *Acta Odontologica Scandinavica, Supplement* **28**, 13–165.
- DELAIRE J, PRECIOUS D (1986) Influence of the nasal septum on maxillonasal growth in patients with congenital labiomaxillary cleft. *Cleft Palate Journal* **23**, 270–277.
- DIETRICH UC (1970) Morphological variability of skeletal class III relationships as revealed by cephalometric analysis. *Report of the Congress of the European Orthodontic Society*, 131–143.
- DIEWERT VM (1983) A morphometric analysis of craniofacial growth and changes in spatial relations during secondary palatal development in human embryos and fetuses. *American Journal of Anatomy* **167**, 495–522.
- DIEWERT VM (1985) Growth movement during prenatal development of human facial morphology. In *Normal and Abnormal Bone Growth, Basic and Clinical Research* (ed. A. D. Dixon & B. G. Sarnat), pp. 57–66. New York: A. R. Liss.
- DUDA RO, HART PE (1973) *Pattern Classification and Scene Analysis*. New York: Wiley and Sons.
- ELLIS E, MCNAMARA JA (1984) Components of adult Class III malocclusion. *Journal of Maxillofacial Surgery* **42**, 295–305.
- GOWER JC (1975) Generalized Procrustes analysis. *Psychometrika* **40**, 33–51.
- GUYER EC, ELLIS EE, MCNAMARA JA, BEHRENTS RG (1986) Components of Class III malocclusion in juveniles and adolescents. *Angle Orthodontist* **56**, 7–30.
- HARRIS E (1993) Size and form of the cranial base in isolated cleft lip and palate. *Cleft Palate–Craniofacial Journal* **30**, 170–174.
- HOPKIN GB, HOUSTON WJB, JAMES GA (1968) The cranial base as an aetiological factor in malocclusion. *Angle Orthodontist* **38**, 250–255.
- HORSWELL BB, GALLUP BV (1992) Cranial base morphology in cleft lip and palate. *Journal of Oral Maxillofacial Surgery* **50**, 681–685.
- HOYTE DAN (1991) The cranial base in normal and abnormal skull growth. *Neurosurgery Clinics of North America* **2**, 515–537.
- JACOBSON A, EVANS WG, PRESTON CB, SADOWSKY PL (1974) Mandibular prognathism. *American Journal of Orthodontics* **66**, 140–171.
- JOHNSON RA, WICHERN RA (1982) *Applied Multivariate Statistical Analysis*. Englewood Cliffs, NJ: Prentice-Hall.
- KREIBORG S, PRYDSOE V, DAHL E, FOGH-ANDERSEN P (1976) Calvarium and cranial base in Apert's syndrome: an autopsy report. *Cleft Palate Journal* **13**, 296–303.
- LATHAM RA (1970) Maxillary development and growth: the septo-premaxillary ligament. *Journal of Anatomy* **107**, 471–478.
- LELE S (1993) Euclidean distance matrix analysis (EDMA): estimation of mean form and mean form difference. *Mathematical Geology* **25**, 573–602.
- LOZANOFF S (1992) Accuracy and precision of computerized models of the anterior cranial base in young mice. *Anatomical Record* **234**, 618–624.
- LOZANOFF S (1993) Midfacial retrusion in adult Brachyrrhine mice. *Acta Anatomica* **147**, 125–132.
- LOZANOFF S, DIEWERT VM (1989) A computer graphics program for measuring two- and three-dimensional form change in developing craniofacial cartilages using finite element methods. *Computers and Biomedical Research* **22**, 63–82.
- LOZANOFF S, DEPTUCH JJ (1991) Implementing Boissonnat's approach for generating surface models of craniofacial cartilages. *Anatomical Record* **229**, 556–564.
- LOZANOFF S, ZINGESER M, DIEWERT VM (1993) Computerized modelling of nasal capsular morphogenesis in prenatal primates. *Clinical Anatomy* **6**, 37–47.
- LOZANOFF S, JURECZEK S, FENG T, PADWAL R (1994) Anterior cranial base morphology in mice with midfacial retrusion. *Cleft Palate–Craniofacial Journal* **31**, 417–428.
- MA W, LOZANOFF S (1993) External craniofacial features, body size and renal morphology in prenatal Brachyrrhine mice. *Teratology* **47**, 321–332.
- MCALARNEY ME, DASGUPTA G, MOSS ML, MOSS-SALENTIUN L (1991) Boundary elements and finite elements in biological morphometrics: a preliminary computation comparison. In *Computers in Biomedicine* (ed. K. D. Held, C. A. Brebbia & R. D. Ciskowski), pp. 61–72. Boston: Computational Mechanics.
- MCALARNEY ME, DASGUPTA G, MOSS ML, MOSS-SALENTIUN L (1992) Anatomical macroelements in the study of craniofacial rat growth. *Journal of Craniofacial Genetics and Developmental Biology* **12**, 3–12.
- MOONEY MP, SIEGEL MI, KIMES KR, TODHUNTER JS (1989) A test of two midfacial growth models using path analysis of normal human fetal material. *Cleft Palate Journal* **26**, 93–99.
- MOONEY MP, SIEGEL MI, KIMES KR, TODHUNTER JS (1991) Premaxillary development in normal and cleft lip and palate human fetuses using three-dimensional computer reconstruction. *Cleft Palate Journal* **28**, 49–53.
- MOSS ML, GREENBERG SN (1955) Postnatal growth of the human skull base. *Angle Orthodontist* **25**, 77–84.
- OUSTERHOUT DK, MELSEN B (1982) Cranial base deformity in Apert's syndrome. *Plastic and Reconstructive Surgery* **69**, 254–263.
- ROHLF FJ, SLICE D (1990) Extensions of the Procrustes method for the optimal superimposition of landmarks. *Systematic Zoology* **39**, 40–59.
- ROSS RB (1965) Cranial base in children with lip and palate clefts. *Cleft Palate Journal* **2**, 157–166.
- ROSS RB (1987) Treatment variables affecting growth in complete unilateral cleft lip and palate: parts 1–7. *Cleft Palate Journal* **24**, 5–77.
- RUDÉ FP, ANDERSON L, CONLEY D, GASSER RF (1994) Three-dimensional reconstructions of the primary palate region in normal human embryos. *Anatomical Record* **238**, 108–113.
- SAMESHIMA GT, MELNICK M (1994) Finite element-based cephalometric analysis. *Angle Orthodontist* **64**, 343–350.
- SANBORN RT (1955) Differences between the facial skeletal patterns of Class III malocclusion and normal occlusion. *Angle Orthodontist* **25**, 208–222.
- SANDHAM A, CHENG L (1988) Cranial base and cleft lip and palate. *Angle Orthodontist* **58**, 163–168.
- SARNAT BG (1970) The face and jaws after surgical experimentation with the nasoseptovomer region in growing and adult rabbits. *Acta Otolaryngologica (Suppl.)* **268**, 1–47.
- SARNAT BG (1991) Normal and abnormal growth of the nasoseptovomer region. *Annals of Otolaryngology and Laryngology* **100**, 508–515.
- SCOTT JH (1953) The cartilage of the nasal septum. *British Dental Journal* **95**, 37–43.
- SEARLE AG (1966) New mutants. *Mouse News Letters* **35**, 27.
- SIEGEL MI, TODHUNTER JS (1979) Image recognition and reconstruction of cleft palate histological preparations: a new approach. *Cleft Palate Journal* **16**, 381–384.
- SIEGEL MI, MOONEY MP, EICHBERG JW, GEST T, LEE DR (1991) Septopremaxillary ligament resection and midfacial growth in a chimpanzee animal model. *Journal of Craniofacial Surgery* **1**, 182–186.
- SIEGEL MI, MOONEY MP, EICHBERG JW, GEST T, LEE DR (1992) Nasal capsule shape changes following septopremaxillary ligament resection in a chimpanzee animal model. *Cleft Plate Journal* **29**, 137–142.
- SINGH GD, MCNAMARA JA, MCGILL JS, LOZANOFF S (1995) Thin-



- plate spline analysis of Class III cranial base morphology. *Journal of Dental Research* **74**, 580.
- STAPF WC (1948) A cephalometric roentgenographic appraisal of the facial pattern in Class III malocclusions. *Angle Orthodontist* **18**, 20–23.
- THEILER K (1989) *The House Mouse Atlas of Embryonic Development*. New York: Springer.
- TROTMAN C-A, ROSS RB (1993) Craniofacial growth in bilateral cleft lip and palate: ages six years to adulthood. *Cleft Palate–Craniofacial Journal* **30**, 261–273.
- VAN LIMBORGH J (1970) A new view on the control of the morphogenesis of the skull. *Acta Morphologica Neerlando-Scandinavica* **8**, 143–160.
- VAN LIMBORGH J (1972) The role of genetic and local environment factors in the control of postnatal craniofacial morphogenesis. *Acta Morphologica Neerlando-Scandinavica* **10**, 37–47.
- WITT PD, HARDESTY RA, ZUPPAN C, ROUSE G, HASSO AN, BOYNE A (1992) Fetal Kleeblattschädel cranium: morphologic, radiographic and histological analysis. *Cleft Palate–Craniofacial Journal* **29**, 363–368.